THE ASTROPHYSICAL JOURNAL, 174:557–572, 1972 June 15

A PHOTOMETRIC STUDY OF THE OPEN CLUSTER NGC 2477

F. D. A. HARTWICK*
University of Victoria, Victoria, British Columbia

JAMES E. HESSER
Cerro Tololo Inter-American Observatory†

AND

ROBERT D. MCCLURE*
Yale University Observatory
Received 1971 November 11; revised 1972 January 10

ABSTRACT

A photometric study of NGC 2477 based on the combined results of photoelectric and photographic *UBV* photometry and intermediate-band photometry on the David Dunlap Observatory (DDO) system has yielded the following results:

1. A differential reddening across the cluster ranging from $E_{B-V} = 0.2$ to $E_{B-V} \simeq 0.4$ mag.
2. A relative metallicity of approximately 1.5 times that of the Hyades.
3. A deficiency of stars on the evolved main sequence between apparent magnitudes $13.87 \lesssim V \lesssim 14.10$.
4. A true distance modulus of $(m - M)_0 = 10.61 \pm 0.21$.
5. Comparison between theoretical model computations and the observed features of the color-magnitude diagram yields an age of $1.5 \pm 0.2 \times 10^9$ years.
6. A group of stars lying above and blueward of the turnoff point. These stars have apparently lower surface gravities than main-sequence stars.

I. INTRODUCTION

NGC 2477 ($\alpha = 7^h48^m.7$, $\delta = -38°17'$, 1950; $l = 254°$, $b = -6°$) is one of the richest open clusters known. It was most recently studied by Eggen and Stoy (1961, hereinafter referenced as ES) who constructed a photoelectrically calibrated color-magnitude (C-M) diagram of the cluster and found it to be of intermediate age. They found a reddening of $E_{B-V} = 0.25$ mag from the main-sequence stars, and later Eggen (1963) determined a reddening of 0.33 mag from the giants alone. Using this latter value of reddening, Eggen concluded that the main-sequence stars had an ultraviolet excess. An important result of ES's work was the discovery of a gap on the evolved main sequence. This was the first time such a gap had been noted.

Our purpose in reinvestigating this cluster was several-fold: to determine unambiguously the reddening and relative metallicity of the cluster stars; to delineate photoelectrically the gap in the evolving main sequence so that a comparison with theoretical evolutionary calculations could be made; and, finally, to measure photographically many more stars with the aim of extending the main sequence to well below the turnoff point, thereby enabling an accurate determination of the distance modulus to be made.

II. OBSERVATIONAL DATA

a) Photoelectric UBV Observations of the Main-Sequence Stars

Photoelectric *UBV* photometry was carried out for a representative sample of the stars on the main sequence of NGC 2477 to define accurately any features present, such

* Visiting Astronomer, Cerro Tololo Inter-American Observatory.

† Operated by the Association of Universities for Research in Astronomy, Inc., under contract with the National Science Foundation.

as the gap found by ES. The photometry was done on the 60-inch (152 cm) and 36-inch (91 cm) telescopes on Cerro Tololo with a conventional photoelectric photometer using an RCA 1P21 photomultiplier and standard *UBV* filters as defined by Johnson (1962). Red leak measurements were subtracted from the *U* deflections. The primary standards used were from the lists of Cousins and Stoy (1963) and Cousins, Lake, and Stoy (1966) and were so chosen that (i) all stars are from equatorial regions; (ii) at least one red and one blue star is found in each 2-hour interval of right ascension; (iii) $+5 < V < +6.5$; and (iv) $|\Delta V| \leq 0.02$ mag, $|\Delta(B - V)| \leq 0.02$ mag, and $|\Delta(U - B)| \leq 0.04$ mag, where the differences are formulated with the magnitudes and colors tabulated by Blanco *et al.* (1968). The extinction coefficients used were mean values determined on at least six nights. Median *internal* standard errors are ± 0.008 in V, ± 0.009 in $(B - V)$, and ± 0.009 in $(U - B)$. The results are tabulated in table 1 for 96 stars brighter than $V = 17.8$ mag. Also shown in the table is the number of nights on which each star was observed, as well as photographically determined magnitudes and colors from measurements on four V plates and six B plates. Nine stars in table 1 were also observed photoelectrically by ES. The average differences in the sense (table 1 − ES) are: $+0.063 \pm 0.020$ mag (s.e.) in V, -0.020 ± 0.013 mag (s.e.) in $(B - V)$, and $+0.059 \pm 0.029$ mag (s.e.) in $(U - B)$. We suspect significant systematic differences in V and possibly $(U - B)$ between the two sets of data. This suspected systematic shift in V was also found in the independent *UBV* observations of the giant stars and will be discussed further in the next section. The need for a small correction to the V-magnitudes of early southern photometry such as that of ES has been noted by others (cf. Cousins 1970).

b) DDO and UBV Photoelectric Photometry of the Red Giants

Twenty-six of the red giant stars in NGC 2477 were observed on the David Dunlap Observatory (DDO) intermediate-bandpass photometric system. This filter system is defined by McClure and van den Bergh (1968) and McClure (1971), and the reader is referred to those papers for a description of the filter bandpasses; only the four filters in the blue spectral region were used.

The photometry was done using the same telescopes and equipment described in § II*a* and DDO filter set D from Yale University Observatory. Linear transformations were made to the original DDO system using standards that are situated near the celestial equator and included in the papers by McClure and van den Bergh (1968) and McClure (1970), as well as for a few southern stars observed at Cerro Tololo by Goodenough (1969). Mean extinction coefficients were used.

The DDO observational data for the NGC 2477 giants are listed in the first four columns of table 2. The color indices listed here will be described in the next section.

Nineteen of the giants were also observed on the *UBV* system with the standard Cerro Tololo equipment and filters described in § II*a*. Red leak measurements were applied in the same manner as described previously. Linear transformations to the *UBV* system were made using E-region standards (Cousins and Stoy 1962; Cousins 1967). The small corrections suggested by Johnson *et al.* (1966) were applied to Cousin's V-magnitudes and $(B - V)$ colors. Mean extinction coefficients were used.

The *UBV* observational data for the cluster giants are listed in columns (6), (7), and (8) of table 2. All magnitudes and color indices listed in table 2 are means of observations from two separate nights except as noted.

Median internal standard errors as determined from multiple observations of stars on separate nights are: ± 0.007 in $C(45 - 48)$, ± 0.010 in $C(42 - 45)$, ± 0.010 in $C(41 - 42)$, ± 0.007 in V, ± 0.008 in $(B - V)$, and ± 0.019 in $(U - B)$. Since all of the giants have V and $B - V$ observations (photographically smoothed) listed by ES, a comparison can also be made with their data. The mean difference in V and $(B - V)$ of this paper minus the ES values is $+0.117 \pm 0.014$ (s.e.) and $+0.003 \pm 0.009$ (s.e.),

TABLE 1

UBV Photometry of Photoelectrically Observed Stars

Star No.		Photoelectric			n	E_{B-V}	Photographic	
H^2M	ES	V	B-V	U-B			V	B-V
A		15.23	0.81	0.24	2		15.19	0.86
B		13.99	0.63	0.35	2	0.36	13.98	0.62
C		13.68	0.64	0.38	2	0.38	13.67	0.69
E		14.86	0.72	0.29	3	0.37	14.83	0.73
F		14.04	0.67	0.40	3	0.41	14.04	0.67
G		14.55	0.71	0.27	3	0.35	14.52	0.73
H		13.25	0.58	0.37	2	0.35	13.28	0.59
J		13.19	0.81	0.46	2	0.53	13.16	0.84
L		13.92	0.62	0.34	2	0.35	13.86	0.65
N		14.09	0.66	0.33	2	0.36	14.13	0.65
O		13.40	0.54	0.38	2	0.35	13.36	0.57
P		13.43	0.61	0.38	2	0.37	13.39	0.59
Q		14.49	1.89		1		14.27	2.29
R		14.06	0.63	0.30	2	0.33	14.01	0.67
S		13.87	0.82	0.36	2	0.47	13.74	0.89
T		13.57	0.63	0.37	2	0.37	13.55	0.64
U		13.63	0.69	0.20	2		13.58	0.72
V		13.80	0.66	0.44	3	0.44	13.76	0.67
W		13.93	0.65	0.39	3	0.40	13.86	0.70
X		13.38	0.58	0.41	2	0.39	13.37	0.53
Y		13.82	0.61	0.35	2	0.35	13.84	0.56
Z		11.62	1.19	0.89	3		11.54	1.23
a		10.51	0.99	0.65	3		10.49	0.99
b		13.41	0.59	0.36	2	0.34	13.42	0.57
c		14.74	0.66	0.23	2	0.29	14.76	0.63
d		14.30	0.70	0.34	2	0.39	14.28	0.71
f		13.34	0.73	0.21	2		13.31	0.75
g		12.23	1.19	0.93	3		12.20	1.23
h		11.36	1.06	0.71	3		11.37	1.01
i		10.84	0.68	0.42	3		10.94	0.61
j		11.46	1.44	1.45	3		11.51	1.46
k		13.15	0.55	0.34	3	0.31	13.20	0.45
l		14.01	0.61	0.29	3	0.31	14.04	0.54
m		12.62	0.57	0.32	1	0.31	12.66	0.52
n		13.38	0.80	0.37	3	0.46	13.39	0.84

Star No.		Photoelectric			n	E_{B-V}	Photographic	
H^2M	ES	V	B-V	U-B			V	B-V
p		13.79	0.63	0.35	2	0.36	13.80	0.63
q		16.59	1.03	0.43	2		16.57	1.11
r		11.32	1.43	1.44	6		11.34	1.40
s		13.44	0.66	0.27	2	0.32	13.49	0.66
t		13.04	0.52	0.35	3	0.31	13.09	0.46
u		14.40	0.60	0.23	3	0.27	14.44	0.56
v		12.86	0.74	0.41	2	0.46	12.90	0.69
w		13.51	0.60	0.36	3	0.35	13.56	0.54
x		12.85	0.50	0.34	2	0.29	12.93	0.40
y		14.55	0.63	0.17	2	0.23	14.57	0.57
z		12.89	0.50	0.29	2	0.25	12.96	0.42
γ		11.61	1.23	0.98	2		11.63	1.25
δ		15.07	0.69	0.28	1	0.34	15.11	0.71
ε		12.04	1.28	1.16	3		11.97	1.38
ζ		14.35	0.66	0.30	2	0.34	14.35	0.67
π		13.13	0.55	0.36	2	0.33	13.17	0.53
σ		10.72	0.17	0.05	4			
φ	116	13.85	-0.16	-1.02	14			
ξ		10.83	0.96	0.59	4			
Ω		14.27	0.66	0.32	2	0.36		
Σ		14.71	0.70	0.31	2	0.37		
λ		11.40	1.55	1.68	4			
1051	750	14.34	0.63	0.24	2	0.29	14.33	0.65
1064	398	13.59	0.66	0.12	4		13.58	0.67
1069	399	9.81	1.88	2.28	13			
1071	739	13.86	0.64	0.27	1	0.31	13.85	0.66
1078		13.27	0.54	0.36	4	0.32	13.31	0.50
1080		14.57	0.62	0.24	2	0.28	14.56	0.66
2049		14.16	1.14	1.21	1		14.04	1.33
2054		13.84	0.58	0.29	2	0.28	13.84	0.61
2064		12.21	1.20	1.00	4		12.22	1.25
2068		13.79	0.56	0.29	2	0.28	13.81	0.57
2077		14.63	0.68	0.26	2	0.33	14.62	0.69
3023		13.09	0.51	0.26	2	0.24	13.08	0.53
3027		13.58	0.51	0.34	3	0.29	13.59	0.53

Star No.		Photoelectric			n	E_{B-V}	Photographic	
H^2M	ES	V	B-V	U-B			V	B-V
3034		13.27	0.48	0.32	2	0.27	13.27	0.47
3059		15.18	0.67	0.13	2		15.21	0.58
3060		14.80	0.68	0.26	3	0.33	14.66	0.68
4019		14.03	0.57	0.24	2	0.26	14.04	0.57
4031		14.22	0.58	0.25	2	0.27	14.24	0.57
4032		14.46	0.69	0.29	2	0.35	14.47	0.65
4034		14.18	0.60	0.24	2	0.27	14.23	0.55
4042		14.13	0.60	0.25	3	0.28	14.17	0.56
4043		14.60	0.70	0.25	2	0.33	14.63	0.68
4045		14.08	0.68	0.21	3	0.28	14.08	0.63
5019		17.04	0.92	0.31	2		17.01	0.96
5020		14.19	0.66	0.21	4	0.27	14.23	0.63
5025		16.35	0.89	0.31	2		16.34	0.86
5035		12.27	1.20	0.99	3		12.28	1.25
5042		15.62	0.86	0.28	4		15.68	0.81
5047	644	11.61	1.25	1.07	7		11.57	1.22
5066		13.56	0.59	0.29	4	0.30	13.62	0.58
5068		17.04	1.09	0.39	2		17.05	1.07
5071	683	14.25	0.58	0.26	1	0.27	14.27	0.61
5102		17.40	0.66	0.51	2		17.53	0.52
5103		17.81	1.09	0.79	2		17.73	1.17
6025		13.38	0.59	0.29	2	0.30	13.36	0.61
6029		12.84	0.55	0.32	2	0.30	12.84	0.53
6040		11.88	1.00	0.76	3		11.85	1.01
6069	532	13.37	0.94	0.49	2		13.17	0.92
6073		13.59	0.48	0.26	2	0.22	13.63	0.46
6086		14.63	0.65	0.18	2	0.24	14.64	0.60
7007	575	11.94	0.58	0.34	8		11.98	0.49
8019	419	12.08	1.27	1.00	1		12.07	1.29
8022		14.57	0.83	0.43	3		14.56	0.81
8046		13.34	0.64	0.34	2	0.36	13.33	0.64
8061		16.19	0.80	0.25	3		16.17	0.79
8067		13.67	0.62	0.39	2	0.38	13.63	0.65
8069		13.65	0.43	0.34	2		13.63	0.43
8073		13.44	0.52	0.32	2	0.26	13.41	0.40

TABLE 2

PHOTOELECTRIC DATA FOR THE RED GIANTS

Star ES	Star H^2M	C(45-48)	C(42-45)	C(41-42)	V	B-V	U-B	E(B-V)	C (42-48)††	C_m(41-42)††
77	ψ	1.214	0.940	0.194	12.47	1.24	0.99	0.32*	1.96	0.31
201	Z	1.237	0.863	0.162	11.66	1.20	0.90	0.28	1.94	0.17
215	e	1.220	0.902	0.195	12.76	1.22	0.96	0.30	1.94	0.26
270	I	1.238	0.852	0.246	12.05	1.22	0.89	0.33	1.89	0.26
272	8039	1.232	0.883	0.220	12.33	1.20	0.95	0.26	1.96	0.24
396	8077	1.255	0.917	0.242	12.18†	1.23†	1.02†	0.29	2.00	0.26
418	1025	1.232	0.825	0.210				0.32***	1.86	0.21
419	8019	1.263	0.889	0.269	12.11†	1.26†	1.07†	0.32	1.96	0.26
430	8018	1.246	0.916	0.245				0.29	1.99	0.28
431	8017	1.207	0.907	0.209	12.57†	1.17†	0.89†	0.22	1.98	0.28
644	5047	1.262	0.921	0.294				0.23	2.05	0.28
695	4067	1.316	1.054	0.332	11.41	1.42	1.36	0.29	2.20	0.35
696	4064	1.232	0.878	0.238	12.55	1.20	0.98	0.28	1.95	0.26
708	4004	1.242	0.872	0.246	10.81†	1.24†	0.98†	0.35	1.91	0.27
752	1044	1.292	0.950	0.360	11.81	1.28	1.07	0.26	2.09	0.33
882	4037	1.242	0.930	0.204	11.96	1.21	0.96	0.19	2.06	0.22
911	D	1.198	0.801	0.200	12.28	1.18	0.81	0.26*	1.84	0.22
913	K	1.229	0.834	0.199	12.63	1.25	0.83	0.33*	1.87	0.21
915	θ	1.328	1.050	0.317	11.49	1.44	1.30	0.31	2.19	0.32
917	M	1.356	1.097	0.356				0.29**	2.28	0.34
920	λ	1.364	1.125	0.374	11.42	1.58	1.63	0.40	2.26	0.40
937	β	1.243	0.888	0.268	11.96	1.22	1.00	0.27	1.97	0.28
938	α	1.233	0.874	0.267	11.85	1.20	0.96	0.28	1.94	0.28
956	r	1.324	1.047	0.372				0.31	2.19	0.38
959	o	1.260	0.924	0.200				0.29**	2.01	0.22
991	h	1.180	0.757	0.162				0.26	1.78	0.17

* Reddening determined from position with respect to giant sequence in HR diagram (Fig. 7b)

** No B-V color. Average reddening $0^m.29$ used.

*** No B-V color. Reddening of nearby star #419 used.

† Observed on one night only.

†† Unreddened values.

respectively. As shown in § II*a* for the main-sequence stars, there appears to be a significant systematic difference between the *V*-magnitudes reported in this paper and those of ES. To check further on this difference a comparison can be made using some stars from a different cluster that were observed on the same nights as the NGC 2477 giants. These additional stars include 15 stars of a photoelectric sequence in the cluster NGC 5822 published by Brück, Smyth, and McLachlan (1968). They range in *V*-magnitude from 9.0 to 12.6, and about half are red giants similar to the NGC 2477 giants. The mean difference in *V* of the stars observed in the present observing run minus those published by Brück *et al.* is -0.011 ± 0.005. This good agreement—along with the fact that similar systematic differences with ES were found for both the giants and main-sequence stars in NGC 2477 even though they were observed on many different observing runs spread over two seasons using different sets of standard filters, photomultiplier tubes, and *UBV* standard stars—indicates that the *V*-magnitudes reported here are likely correct.

c) Photographic Observations

Photographic observations of over 2000 stars in NGC 2477 were made in order to delineate the principal sequences in the C-M diagram. Only those stars in the central ring of ES were tabulated and included in the following discussion when it became apparent that a large differential reddening was contributing to the scatter. For 229 of these stars with $V < 15$ and $(B - V) < 0.9$ we measured four *V* plates (103aD) + GG14) and six *B* plates (103aD + GG13). The remaining 453 stars were measured on only one plate pair. The plate material was obtained with the f:7.5 Ritchey-Chrétien focus of the 60-inch telescope on Cerro Tololo. A calibration curve consisting of a computer-fitted, sixth-degree polynomial was constructed for each plate separately. Median values of the standard errors for the multiply observed stars are ± 0.020 mag in *V* and ± 0.025 mag in $(B - V)$. These stars are identified in figure 1 (plate 2) and the data given in table 3. Photographic observations of the standard stars are given in table 1. A

TABLE 3

PHOTOGRAPHIC DATA

Star	V	B-V	Star	V	B-V	Star	V	B-V	Star	V	B-V	Star	V	B-V
1001	15.75	0.71	1080	14.56	0.66	2074	17.04	0.94	3068	16.04	1.11	4064	12.51	1.23
1002	13.23	0.53	1081	17.69	0.66	2075	15.37	0.70	3069	16.91	1.27	4065	17.62	0.69
1003	13.63	0.54	1082	17.57	0.84	2076	15.51	0.76	3070	15.61	1.48	4066	17.00	1.32
1004	15.90	0.92	1083	16.22	1.00	2077	14.62	0.69	3071	15.45	0.74	4067	11.32	1.44
1005	16.38	0.93	1084	15.03	0.98	2078	14.97	0.70	3072	12.00	1.19	4069	15.96	1.01
1007	12.79	0.55	1085	16.92	0.95	2079	16.69	0.94	3073	16.86	0.85	4071	13.36	0.28
1008	12.24	1.08	2001	12.43	0.44	2080	16.95	1.13	3074	16.95	1.25	4072	15.95	0.87
1009	16.88	0.84	2002	16.44	0.77	2081	12.72	0.75	3076	15.97	0.43	4073	13.39	0.48
1010	15.25	0.58	2003	14.19	0.51	2082	17.20	0.97	3077	12.82	0.48	4074	15.71	0.94
1011	14.26	0.56	2004	16.17	1.28	3001	13.63	0.54	3078	15.03	0.70	4075	15.80	0.96
1012	14.80	0.65	2005	14.54	0.71	3002	12.79	0.55	3079	17.39	0.97	4076	17.23	1.12
1013	15.74	0.97	2006	13.26	0.49	3003	12.31	1.08	3080	15.70	1.30	4077	17.18	1.14
1014	12.23	1.22	2007	12.07	0.44	3004	11.68	0.35	3081	17.55	0.65	4078	15.93	1.03
1015	14.87	0.64	2008	13.91	0.67	3005	14.93	0.58	3082	17.48	0.75	4079	15.26	1.13
1016	13.57	-0.09	2009	10.81	1.59	3006	16.10	0.82	3083	16.17	0.91	4080	15.28	0.74
1017	17.24		2010	16.86	0.96	3007	16.82	0.98	3084	17.34	0.72	4081	12.60	0.62
1018	14.48	0.50	2011	17.13	0.71	3008	13.44	1.46	3085	15.73	0.74	4082	15.93	0.89
1019	16.35	0.89	2012	14.84	0.63	3009	13.83	0.57	4001	14.36	0.61	4083	14.31	0.55
1020	12.95	0.59	2013	17.25	0.87	3010	16.77	0.74	4002	14.78	0.72	4084	14.58	1.26
1021	12.40	0.53	2014	15.14	0.71	3011	15.52	0.77	4003	15.08	0.69	5001	16.41	0.87
1022	14.14	0.61	2015	15.17	0.90	3012	14.92	0.66	4004	10.73	1.16	5002	14.43	0.63
1023	16.96	1.03	2016	14.54	0.60	3013	17.53	0.74	4005	16.53	0.95	5003	14.78	0.63
1024	13.29	0.52	2017	16.99	0.96	3014	12.85	0.64	4006	16.36	0.94	5004	14.81	0.66
1025	12.26	1.25	2019	17.25	0.96	3015	16.21	0.90	4007	15.08	0.64	5005	16.31	0.98
1026	12.69	0.75	2020	14.35	0.85	3016	16.28	0.53	4008	15.88	0.87	5007	15.72	0.89
1027	16.04	0.74	2021	12.94	0.53	3017	16.41	1.05	4009	12.52	0.37	5009	16.49	1.03
1028	15.14	0.70	2022	13.49	0.51	3018	14.33	0.87	4010	17.21	1.01	5011	16.07	0.76
1029	15.83	0.89	2023	15.24	0.78	3019	12.90	0.46	4011	12.92	0.44	5012	17.19	1.07
1030	13.17	0.54	2024	10.89	0.53	3020	15.24	0.77	4012	13.10	1.72	5013	14.57	0.77
1031	12.91	0.64	2025	16.16	0.78	3021	17.24	0.74	4013	13.27	0.45	5014	15.28	0.65
1032	15.10	0.69	2026	12.88	0.56	3022	13.67	0.57	4014	17.41	0.42	5015	15.10	0.74
1033	10.67	0.78	2027	16.12	0.77	3023	13.08	0.53	4015	16.70	1.27	5016	12.11	0.31
1034	15.49	0.77	2028	17.23	1.07	3024	15.73	1.23	4016	16.68	1.34	5017	11.70	0.35
1035	14.90	0.65	2029	14.07	0.61	3025	15.68	0.75	4017	16.69	0.95	5018	14.12	0.73
1036	14.01	0.57	2030	13.58	0.57	3026	14.88	0.63	4018	17.25	1.00	5019	17.01	0.96
1037	17.44	0.82	2031	17.36	0.71	3027	13.59	0.53	4019	14.04	0.57	5020	14.23	0.63
1038	14.87	0.80	2032	17.39	0.91	3028	16.24	1.20	4020	16.41	0.96	5021	16.02	0.85
1039	14.41	0.75	2033	14.16	0.62	3029	16.75	1.43	4022	17.40	0.87	5022	17.24	1.01
1040	14.71	0.69	2034	15.80	0.95	3030	17.27	0.73	4023	12.95	0.54	5023	15.72	0.93
1041	17.55	0.87	2035	12.93	0.50	3031	16.01	1.60	4024	15.11	0.67	5024	15.98	0.85
1042	15.85	0.90	2036	11.95	1.27	3032	13.20	0.58	4025	16.94	1.14	5025	16.34	0.86
1043	16.80	1.40	2037	12.91	0.51	3033	16.63	0.79	4026	16.33	1.45	5026	16.76	0.83
1044	11.70	1.36	2038	15.55	0.30	3034	13.27	0.47	4027	12.07	1.18	5027	12.29	0.38
1045	15.53	0.98	2039	17.34	0.79	3035	15.78	0.74	4028	13.10	0.43	5028	13.16	0.46
1046	14.31	0.67	2040	15.11	0.26	3036	12.44	0.65	4029	17.62	0.70	5029	12.85	0.65
1047	13.69	0.68	2041	15.94	0.97	3037	17.45	0.88	4030	17.20	0.96	5030	13.54	0.47
1048	16.21	0.85	2042	12.32	0.18	3038	14.06	0.54	4031	14.24	0.57	5031	13.64	0.48
1050	17.56	0.80	2043	16.23	0.83	3039	15.97	1.00	4032	14.47	0.65	5032	17.18	0.86
1051	14.33	0.65	2044	16.56	0.72	3040	13.75	0.54	4033	14.80	0.69	5033	14.74	1.43
1052	17.30	0.69	2045	16.35	0.86	3041	16.69	1.43	4034	14.23	0.55	5034	13.40	0.52
1053	16.94	0.94	2046	14.42	0.63	3042	14.46	0.64	4035	11.69	2.06	5035	12.28	1.25
1054	16.08	0.58	2047	16.48	0.81	3043	16.60	1.05	4036	16.21	0.53	5036	13.79	0.54
1055	17.60	0.72	2048	14.81	0.68	3044	16.49	0.91	4037	11.94	1.25	5037	15.68	0.90
1056	17.44	0.82	2049	14.04	1.33	3045	12.83	0.41	4038	16.65	0.98	5038	14.15	0.57
1057	12.76	0.43	2050	15.98	0.98	3046	17.41	0.67	4039	16.75	1.13	5039	15.16	1.06
1058	15.30	0.79	2051	13.86	0.59	3047	16.61	0.79	4040	12.51	0.46	5040	15.96	0.97
1059	17.21	1.05	2052	16.75	1.03	3048	15.66	0.78	4041	15.93	0.90	5041	17.07	1.04
1060	15.72	0.79	2053	15.67	0.77	3049	15.67	0.72	4042	14.17	0.56	5042	15.68	0.81
1061	15.11	0.81	2054	13.84	0.61	3050	14.89	0.67	4043	14.63	0.68	5043	12.10	1.16
1062	15.06	0.68	2055	14.68	0.67	3051	15.58	0.70	4045	14.08	0.63	5044	12.61	0.52
1063	16.84	0.94	2057	14.72	0.71	3052	17.21	0.68	4046	11.87	0.93	5045	15.69	0.85
1064	13.58	0.67	2058	13.93	0.52	3053	13.40	0.49	4047	17.05	1.06	5046	14.74	1.43
1065	16.50	1.08	2059	15.59	0.84	3054	16.93	0.82	4049	15.28	0.79	5047	11.57	1.22
1066	14.39	0.66	2060	15.55	0.70	3055	15.11	0.69	4050	17.28	0.93	5048	17.16	0.96
1067	13.26	0.53	2061	12.48	1.21	3056	16.13	0.35	4051	17.27	0.96	5049	15.10	0.64
1068	16.29	0.90	2062	12.35	1.36	3057	15.90	0.78	4052	15.55	0.95	5050	13.43	0.47
1069	9.65	1.95	2063	14.38	0.75	3058	13.58	0.48	4053	16.76	0.91	5051	15.09	0.67
1070	15.24	0.74	2064	12.22	1.25	3059	15.21	0.58	4054	16.61	1.17	5052	12.91	0.40
1071	13.85	0.66	2065	16.72	0.93	3060	14.66	0.68	4055	15.61	0.88	5054	15.45	0.73
1072	17.65	0.62	2066	13.81	0.63	3061	17.41	0.87	4056	17.46	0.76	5055	16.59	0.95
1073	15.88	1.13	2067	15.47	0.72	3062	16.14	0.85	4058	14.02	0.56	5056	17.22	0.87
1074	15.37	0.76	2068	13.81	0.57	3063	12.37	0.49	4059	17.12	1.05	5057	16.69	1.08
1075	16.73	0.99	2069	17.25	0.92	3064	12.74	0.51	4060	16.61	1.00	5058	14.09	0.91
1076	17.19	1.03	2070	14.59	0.64	3065	16.89	1.14	4061	14.18	0.62	5059	15.38	0.70
1078	13.31	0.50	2071	14.23	0.56	3066	17.36	0.99	4062	16.58	0.99	5060	16.03	1.44
1079	17.54	0.71	2073	15.59	0.77	3067	16.46	0.95	4063	13.39	0.52	5061	17.08	0.90

TABLE 3—*Continued*

Star	V	B-V	Star	V	B-V	Star	V	B-V	Star	V	B-V
5063	15.57	0.75	6039	11.41	0.74	7027	12.25	0.44	8006	12.70	0.51
5064	13.50	0.49	6040	11.85	1.01	7028	14.30	0.64	8007	12.78	0.50
5065	12.69	0.47	6041	13.53	0.55	7029	14.14	0.53	8008	15.74	0.89
5066	13.62	0.58	6042	17.04	0.98	7030	14.71	0.59	8009	14.77	0.61
5067	14.91	0.66	6043	17.24	0.78	7031	16.28	0.93	8010	12.62	0.52
5068	17.05	1.07	6044	16.59	1.83	7032	15.71	0.74	8011	14.50	0.61
5070	14.60	0.63	6045	17.16	1.03	7033	16.42	1.04	8012	13.84	0.51
5071	14.27	0.61	6046	14.50	0.55	7034	16.46	0.92	8013	14.33	0.59
5072	15.86	0.90	6047	14.95	0.69	7035	14.06	0.55	8014	15.90	1.09
5073	12.08	1.31	6049	14.76	0.61	7036	15.20	0.71	8015	13.59	0.55
5074	12.28	1.40	6051	17.40	0.68	7037	13.89	0.57	8016	16.57	1.07
5075	16.21	1.04	6052	12.30	0.48	7038	15.45	0.71	8017	12.53	1.25
5076	12.29	1.30	6053	10.75	1.52	7039	15.67	0.80	8018	11.84	1.28
5077	14.92	1.53	6054	12.09	1.06	7040	13.84	0.60	8019	12.07	1.29
5078	14.60	0.66	6055	15.08	0.84	7041	15.70	0.74	8020	16.81	0.69
5079	14.99	0.70	6056	12.70	0.44	7042	16.18	0.83	8021	16.16	0.88
5080	17.34	0.80	6057	15.81	0.81	7043	14.75	0.67	8022	14.56	0.81
5081	16.98	1.01	6058	12.47	1.17	7044	16.18	1.01	8023	12.99	0.60
5082	15.19	0.85	6059	14.52	0.62	7045	14.10	0.54	8026	13.11	0.71
5084	14.90	0.65	6060	16.45	0.97	7046	14.56	0.64	8027	16.53	0.85
5085	17.22	0.99	6061	15.33	0.88	7048	12.68	0.43	8028	12.22	1.16
5086	15.10	0.71	6062	12.09	1.06	7049	12.27	0.57	8029	15.35	1.07
5087	15.79	1.10	6065	17.22	0.78	7050	13.69	0.50	8030	16.18	0.80
5088	15.82	0.91	6066	13.46	0.52	7051	13.41	0.48	8031	16.39	0.90
5089	16.46	0.71	6067	13.47	0.49	7052	14.21	0.59	8032	13.79	0.53
5090	16.33	0.99	6069	13.17	0.92	7053	14.89	0.64	8033	12.32	1.29
5091	13.68	0.49	6070	12.88	0.46	7054	14.09		8034	15.80	0.83
5092	16.34	0.92	6071	15.36	0.65	7056	13.04	0.46	8035	11.99	0.51
5093	14.49	1.08	6072	16.26	1.33	7057	16.68	1.13	8036	17.32	0.70
5094	12.44	1.21	6073	13.63	0.46	7058	13.58	0.93	8037	14.49	0.74
5095	13.77	0.53	6074	17.21	0.92	7059	16.68	1.09	8038	16.70	0.82
5096	14.53	1.34	6075	17.09	1.04	7060	12.46	0.46	8039	12.17	1.18
5097	16.03	1.26	6076	16.81	0.82	7061	14.29	0.69	8040	16.70	1.02
5098	15.89	0.93	6077	17.16	0.89	7062	15.83	1.01	8041	16.37	0.91
5099	14.72	0.60	6078	15.89	0.78	7063	15.78	1.09	8042	15.72	0.86
5100	17.21	0.78	6079	17.42	0.58	7064	12.51	1.19	8043	16.21	0.86
5101	15.43	0.81	6080	15.87	0.85	7066	14.21	0.59	8044	15.32	0.76
5102	17.53	0.52	6081	16.91	0.99	7067	16.18	0.93	8045	16.79	0.98
5103	17.73	1.17	6082	15.76	0.76	7068	16.58	0.99	8046	13.33	0.64
6001	16.48	1.13	6083	14.34	0.57	7069	15.34	0.77	8047	13.98	0.58
6002	13.13	0.52	6084	16.12	0.97	7070	13.24	0.65	8048	13.59	0.53
6003	13.28	0.44	6085	15.05	0.66	7071	12.39	0.59	8049	16.21	0.78
6004	13.06	0.46	6086	14.64	0.60	7072	14.24	0.66	8050	12.86	0.53
6005	12.40	1.21	6087	13.81	0.66	7073	15.14	0.83	8051	14.27	0.67
6006	15.30	0.66	6088	12.18	1.26	7074	16.26	0.84	8052	13.94	0.52
6007	14.25	0.59	6089	17.24	0.44	7075	16.09	0.95	8053	14.20	0.54
6008	13.67	1.76	6090	14.56	0.64	7076	16.56	1.24	8054	12.34	0.45
6009	16.02	0.82	6091	12.69	0.43	7077	16.25	0.95	8055	16.22	0.90
6010	16.91	0.89	6092	15.16	0.66	7078	16.63	0.74	8056	12.81	0.49
6011	16.32	0.85	6093	15.01	0.68	7079	17.04	0.82	8057	12.74	1.96
6012	15.35	0.79	6094	14.93	0.67	7080	15.50	0.74	8058	15.24	0.91
6013	14.12	0.50	7001	13.17	0.55	7081	15.85	0.90	8059	15.30	0.80
6014	13.34	0.55	7002	16.48	0.95	7082	16.24	0.83	8060	15.92	2.23
6015	15.68	0.80	7003	15.55	0.71	7083	16.86	0.98	8061	16.17	0.79
6016	15.73	0.83	7004	12.95	0.35	7084	14.86	0.56	8062	15.30	0.71
6017	15.52	0.72	7005	16.49	0.92	7085	13.24	0.49	8063	15.46	0.73
6018	14.68	0.75	7006	16.01	1.00	7086	12.61	0.43	8064	15.50	1.59
6019	16.25	1.14	7007	11.98	0.49	7087	13.14	0.49	8065	15.72	0.83
6020	12.35	1.18	7008	14.91	0.67	7088	16.89	0.86	8066	16.21	0.83
6021	13.06	0.42	7009	14.30	0.55	7089	16.03	0.85	8067	13.63	0.65
6022	14.99	0.65	7010	15.44	0.78	7090	14.42	0.71	8068	13.24	0.60
6023	13.78	2.11	7011	12.91	0.52	7091	16.66	1.00	8069	13.63	0.43
6024	15.99	0.90	7012	12.30	1.25	7092	12.71	0.42	8070	16.39	0.73
6025	13.36	0.61	7014	15.38	1.35	7093	17.03	0.91	8071	17.58	0.73
6026	15.04	0.69	7015	12.32	0.60	7094	13.79	1.33	8072	16.49	1.11
6028	14.33	0.71	7016	15.72	0.76	7095	13.40	0.51	8073	13.41	0.40
6029	12.84	0.53	7017	16.35	0.85	7096	12.69	0.52	8074	17.39	0.77
6030	17.66	0.66	7018	16.09	0.87	7097	12.07	0.36	8075	15.16	0.72
6031	17.57	0.76	7019	12.50	0.52	7098	16.47	1.09	8076	12.98	0.51
6032	14.48	0.66	7020	15.49	0.71	7099	15.87	0.84	8077	12.08	1.31
6033	17.66	0.33	7021	14.89	0.64	7100	16.91	0.76	8078	15.69	1.58
6034	14.76	0.88	7022	13.11	0.48	8001	12.90	0.42	8080	17.29	1.06
6035	15.39	0.77	7023	12.87	0.54	8002	12.43	0.42	8081	15.93	0.91
6036	15.65	0.94	7024	13.06	0.44	8003	15.95	1.06	8082	14.89	0.91
6037	15.91	1.16	7025	13.57	0.50	8004	12.13	0.55	8083	13.14	0.54
6038	13.18	0.57	7026	15.57	1.02	8005	13.53	0.51	8084	15.75	0.81

check was made for color equations in the photographic data, but none were found. We also checked for plate and field errors, and a map showing the residuals (photoelectric minus photographic) is shown in figure 2. There is evidence for a significant systematic deviation in the southern quadrant; however, no corrections have been applied to the data in table 3 since these deviations, if real, appear to be confined to areas farther from the cluster center than the central ring.

III. REDDENING AND METALLICITY

a) The Reddening and Metallicity from DDO Photometry of the Giants

A value of ultraviolet excess is difficult to determine for NGC 2477 from *UBV* observations alone because the interstellar absorption in this region is very large and, as will be shown below, there appears to be differential reddening across the field. The metallicity of the cluster can be inferred, however, from DDO photometry of the giants

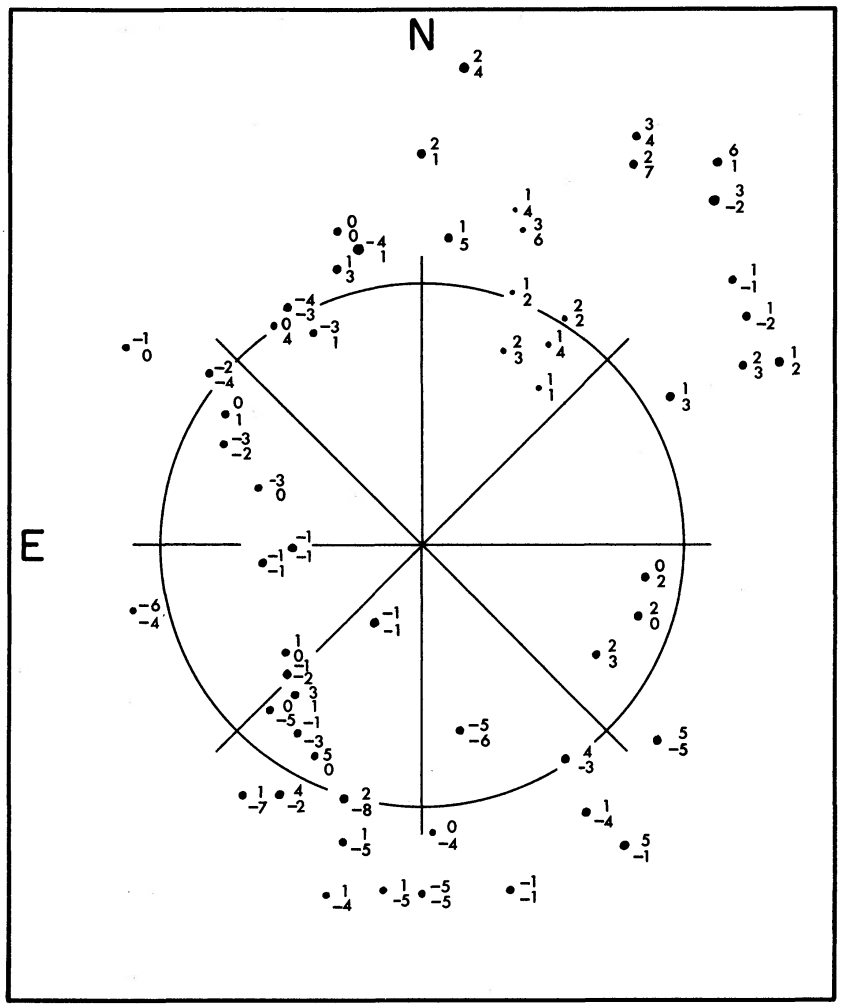

FIG. 2.—A map showing differences of the photometry (pe − pg) versus position in the cluster. The top number for each point is the mean difference in units of 0.01 mag from the *B* plates, and the bottom number is the mean difference from the *V* plates. There is a tendency for differences to be positive in the northwest quadrant and negative in the southern quadrant. The stars measured photographically and plotted in the C-M diagram (fig. 8) are all contained within the ring shown here; and the effects of field errors, if any, are likely to be small. The radius of the circle represents 5 minutes of arc.

after suitable corrections for reddening. The procedures used are described in detail by McClure (1970). From the four intermediate-band observations, three color indices were formed: $C(41 - 42)$, a measure of the strength of the λ4216 cyanogen band; $C(42 - 45)$, an indication of the size of the break in the continuum at the G-band, and $C(45 - 48)$, a color index devoid of strong spectral features. A combination of the latter two indices gives a good measure of temperature and surface gravity, while the cyanogen-band index, after correction for surface gravity, indicates the metallicity.

The reddening was determined for each cluster giant from the observed $(B - V)$ and DDO color indices using the method derived by McClure and Racine (1969). The method takes advantage of the fact that the G-band break index $C(42 - 45)$ has about equal sensitivity to effective temperature as $(B - V)$ whereas the separation in wavelength of the filters is only one-quarter that of the B and V filters. The $(B - V)$ index is therefore about 4 times more affected by interstellar absorption than is $C(42 - 45)$.

The values of color excess determined by DDO photometry are listed in column (9) of table 2. Because the method is suitable only for stars with surface gravities in the luminosity class II to IV range, a few stars had indeterminable reddenings. These and the stars without photoelectric $(B - V)$ colors have reddenings listed that were determined by other means, as noted in the footnotes to table 2. The mean value of $E(B - V) = 0.29$ mag and the large variation therein is in good agreement with values of color excess determined below from UBV colors of the main-sequence stars.

The effects of interstellar reddening on the DDO indices were removed following the procedure outlined by McClure and van den Berg (1968). Only reddening-free indices are plotted in figures 3 and 4.

Since the strength of the cyanogen band is dependent on surface gravity, a correction must be made to the DDO cyanogen index $C(41 - 42)$ before it can be used effectively as a metallicity indicator. This was done following the precepts outlined by McClure (1970) to form the surface-gravity–independent index:

$$C_m(41 - 42) = C(41 - 42) - 1.66[C(45 - 48) - 0.45C(42 - 45) - 0.792] .$$

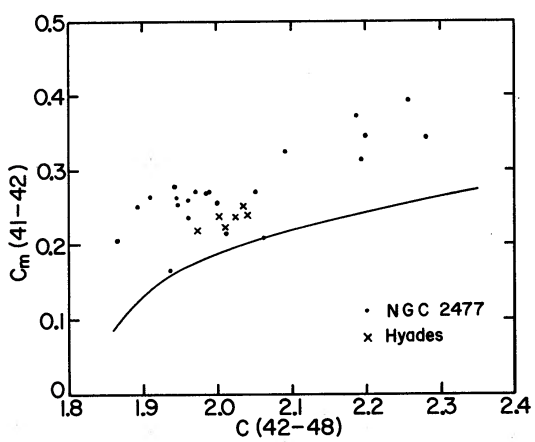

FIG. 3

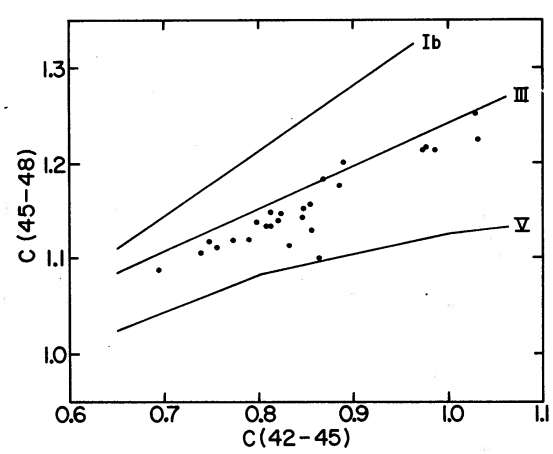

FIG. 4

FIG. 3.—The DDO surface-gravity–corrected cyanogen index $C_m(41 - 42)$ versus the temperature index $C(42 - 48)$. Most of the NGC 2477 giants lie on a locus parallel to the mean relation for solar neighborhood stars (*solid curve*) but shifted by 0.08 mag, thus indicating strong cyanogen bands. The cyanogen excess δC_m is 0.04 mag greater than the Hyades giants, thus indicating a metallicity of about 1.5 times greater if the calibration with [Fe/H] illustrated by McClure (1970) is assumed.

FIG. 4.—The DDO surface-gravity–sensitive index $C(45 - 48)$ versus the temperature-sensitive index $C(42 - 45)$. The NGC 2477 giants appear to have slightly higher surface gravities than solar neighborhood giants (class III line).

This index is shown plotted versus $C(42 - 48)$ in figure 3. The curve is the mean line for solar neighborhood stars, the crosses are the four Hyades cluster giants and two Hyades moving-group giants, and the dots are the NGC 2477 giants. The majority of NGC 2477 giants show cyanogen-band strengths considerably in excess of the Hyades giants. The mean cyanogen excess, δC_m, the vertical distance above the mean line for solar neighborhood stars, is 0.08 mag for the NGC 2477 giants, compared with 0.04 mag for the Hyades giants. Values of δC_m between 0.08 and 0.14 mag are typical of stars classified spectroscopically as "4150" stars by Roman (1952), so the NGC 2477 stars appear to be true examples of strong-cyanogen stars. A possible reason for an anomalously high cyanogen index is an incorrect reddening correction. The mean cyanogen excess δC_m would be high by 0.03 mag if E_{B-V} were erroneously 0.1 mag too large. It is unlikely that the E_{B-V} is in error by nearly this much considering the good agreement between the DDO reddenings and the reddenings determined from *UBV* observations of the main-sequence stars.

The effect of surface gravity can be seen by examining figure 4 where the DDO surface-gravity diagram, $C(45 - 48)$ versus $C(42 - 45)$, is plotted for the NGC 2477 giants. The mean intrinsic relations determined by McClure (1970) for field stars of luminosity classes V, III, and Ib are also shown. The stars appear to have surface gravities that are slightly high with respect to solar neighborhood giants. The sequence in figure 4 lies 0.02 mag below the mean class III line, and therefore the mean correction to the cyanogen index is less than 0.03 mag.

In figure 4 the star lying near the dwarf sequence is ES number 77. This is also the star farthest from the cluster center of all of the giants measured, and the only explanation for its anomalous position in figure 4 is that it might be a foreground subgiant with lower reddening than that used. The other two stars that lie lowest in figure 4, ES numbers 215 and 431, also lie lowest in the C-M diagram of the giant branch, so the high surface gravities indicated in the figure are reasonable.

b) Reddening from UBV Photometry

It is difficult to disentangle reddening and ultraviolet excess from *UBV* observations alone. However, we can infer $\delta(U - B)$ for dwarfs from the DDO photometry as follows. In the previous section we found a mean cyanogen excess of $\delta C_m = +0.04$ over the Hyades value. If figure 2 of Janes and McClure (1971) is used as a calibration, this corresponds to an ultraviolet deficiency for the giants of $\delta(U - B) = -0.03$. Because of higher metallic line blanketing of late-type stars, the slope of the relation between ultraviolet excess and heavy-element abundance is likely to be greater for giants than for dwarfs. This is illustrated by comparing figure 9 of Wallerstein (1962) with figure 2 of Wallerstein and Helfer (1966). Therefore, the ultraviolet deficiency for dwarfs in NGC 2477 corresponding to $\delta(U - B) = -0.03$ for the giants is likely to be near zero.

In principle the reddening can be determined from *UBV* photometry of the main-sequence stars and the metallicity inferred from their ultraviolet excesses. This is possible provided a sufficient number of these stars fall within the intrinsic color range $0.47 < B - V < 0.52$ mag where the reddening line is parallel to the Hyades locus in the two-color plane. Although figure 5 shows relatively few stars in this range, $\delta(U - B) \sim 0$ is consistent with our data and in agreement with the conclusion from DDO photometry. Thus we assumed $\delta(U - B) \sim 0$ and unreddened each of the stars to the Hyades locus. After correcting for reddening, the resulting C-M diagram was compared with that of the Hyades (Johnson and Knuckles 1955). It was found that the evolved main sequences coincided, thus obviating the need for a gravity correction (Eggen and Sandage 1964: figs. 4 and 5). The reddenings obtained are tabulated in table 1, and a reddening map using these reddenings and those found in the previous section for the giants is presented in figure 6. The values found from independent analyses are in accord,

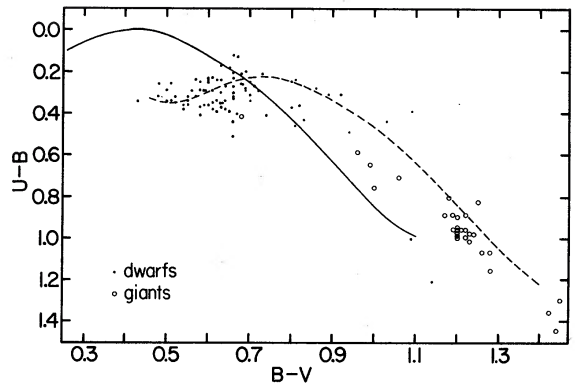

FIG. 5.—The two-color diagram for NGC 2477 stars observed photoelectrically. *Solid curve*, the Hyades intrinsic relation. *Dashed curve*, the Hyades relation shifted for a reddening of $E(B - V) = 0.31$ mag and a color-excess ratio of $E(U - B)/E(B - V) = 0.72$. The ultraviolet deficiency of the giants is due to two factors: (1) the high metallicity of the cluster; (2) the steeper slope of the reddening line for late type stars (Schmidt-Kaler 1961; Fernie 1963; Wildey 1963).

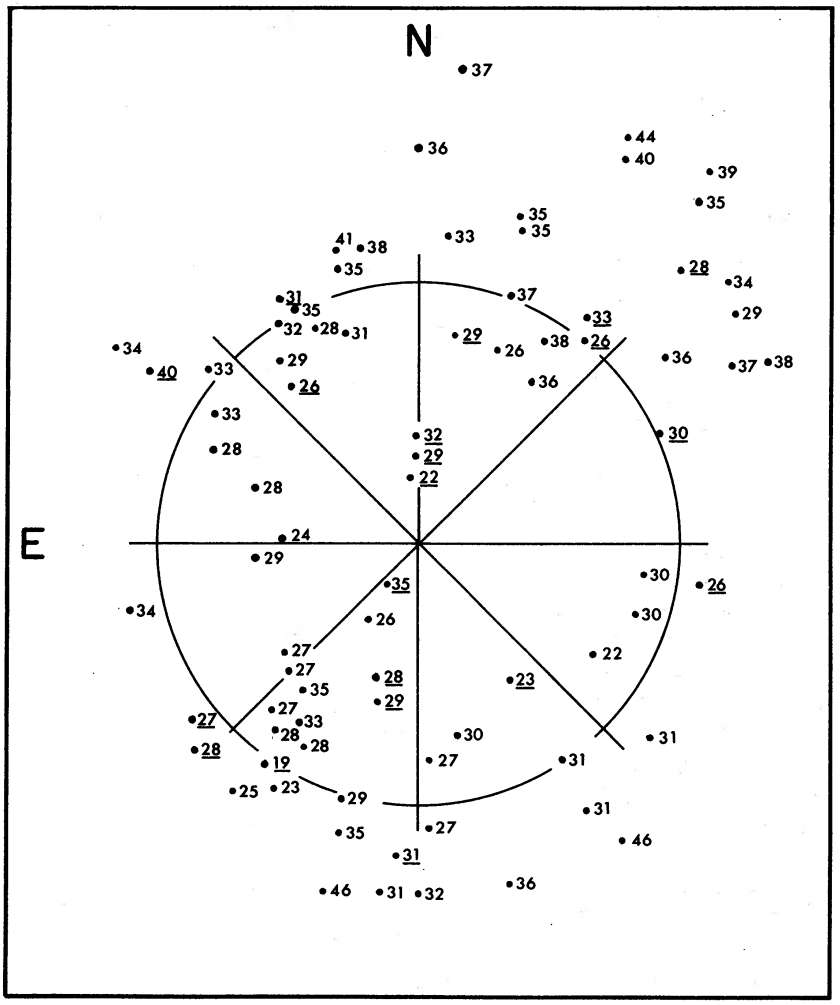

FIG. 6.—A map showing the color excess, $E(B - V)$, versus position in the cluster. The underlined values were deduced from DDO photometry of the giants, while the rest are from *UBV* photometry of main sequence stars. The agreement is good and appears to support the indication of differential reddening across the cluster. The reddening appears to increase toward the northwest and toward the south. The radius of the circle represents 5 minutes of arc.

and we conclude that NGC 2477 is differentially reddened up to ~0.2 mag over the area investigated.

An interesting result concerning reddening of the giant stars can be obtained from inspection of the color-color plot in figure 5. The dashed line in figure 5 represents the Hyades relation shifted for the mean reddening of the photoelectrically observed main-sequence stars, $E(B - V) = 0.31$ mag, and using $E(U - B)/E(B - V) = 0.72$. A much higher ultraviolet deficiency is indicated for the giants than the value $\delta(U - B) = -0.03$, inferred from DDO photometry. Thus, if a color-excess ratio of $E(U - B)/E(B - V) = 0.72$ were used for the giants, a much smaller value of reddening would be obtained for the giant stars than for the main-sequence stars. This supports the important results of Schmidt-Kaler (1961), Wildey (1963), and Fernie (1963) that the reddening line for late-type stars is steeper than the value 0.72 that is commonly used for early-type stars. A second result is that the DDO photometry gave a mean reddening of 0.29 for the giants, just slightly smaller than the mean reddening for the main-sequence stars. This slightly smaller reddening is again in agreement with the results of the above three authors who find that late-type stars should exhibit slightly smaller color excesses than early-type stars that have the same interstellar absorption.

IV. DISCUSSION OF THE C-M DIAGRAM

a) Presentation of the C-M Diagram

The presence of differential reddening in NGC 2477 will tend to mask astrophysically interesting features such as a gap in the main sequence. This smearing effect is well illustrated in figure 7, where the photoelectric data are plotted: (*a*) uncorrected for reddening, and (*b*) corrected for values of the reddening tabulated in tables 1 and 4. Figure 8 is a plot of the photographic data of table 3 and of those stars also lying within the inner ring of ES's figure 2 for which we obtained photoelectric measurements. The random errors were given in § III. If we now include a very pessimistic estimate of plate errors of ± 0.04 mag in $(B - V)$, then the total uncertainty in $(B - V)$ for the multiply observed stars becomes ± 0.05 mag. When account is taken of differential reddening in this area of $\sim\pm 0.05$ mag, we can construct the error box shown on figure 8. Superposition of figure 7*b* on figure 8 yields an average reddening $E_{B-V} = 0.28$ for stars in

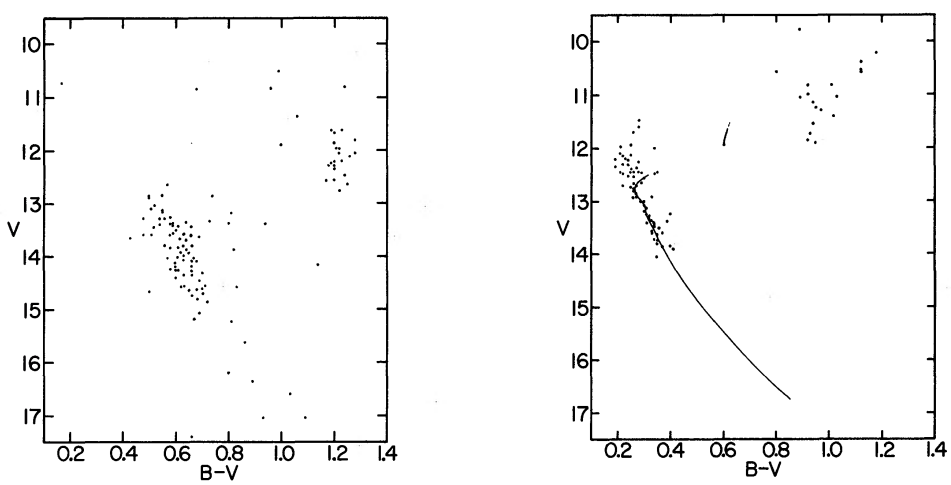

FIG. 7.—(*a*) The observed C-M diagram for stars observed photoelectrically. (*b*) The C-M diagram for the same stars after the application of individual corrections for reddening. The main-sequence stars were unreddened in the $(U - B, B - V)$-diagram to the Hyades locus. The reddenings for the giants were obtained from the DDO photometry. The track indicated by the solid curve is explained in fig. 10.

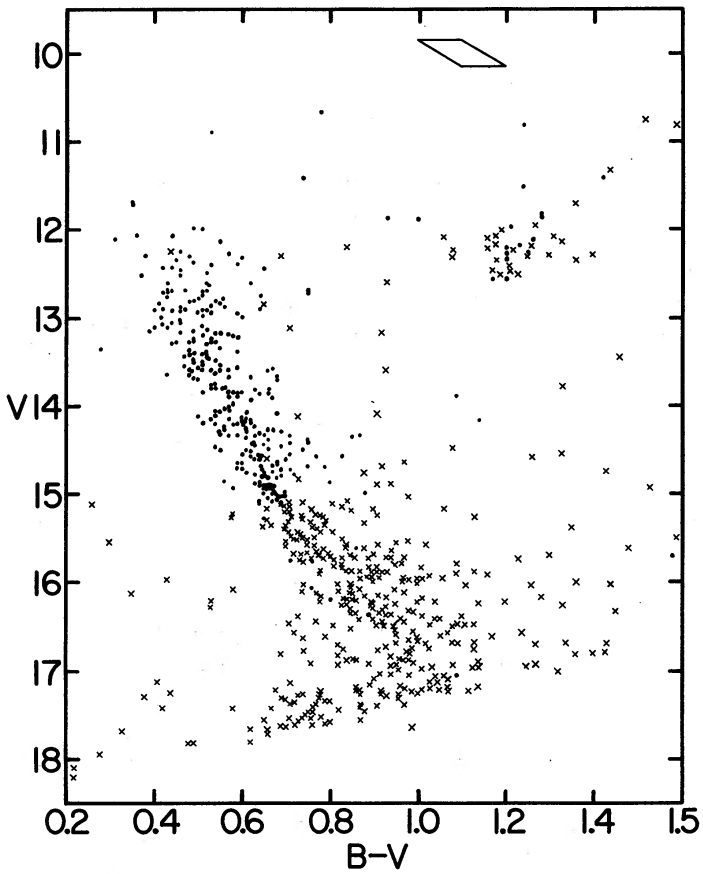

FIG. 8.—The observed C-M diagram for all stars within the central ring of ES. *Dots*, stars measured on six B plates and four V plates. *Crosses*, stars measured on one plate pair only. An error box is shown indicating maximum errors in photometry (*horizontal lines*) and differential reddening (*slanted lines*). Not shown are two stars (1069 and 4035) with $(B - V) \geq 1.9$ which appear to lie on a red extension of the giant branch.

the same region considered by ES; this value compares favorably with those (cf. § I) found by ES and by Eggen (1963).

Of the stars in table 3 which are redder than $(B - V) = 1.5$ and hence are not shown in figure 8, we wish to draw particular attention to stars 1069 and 4035 (ES nos. 399 and 879, respectively) which appear to lie on a red extension of the giant branch in NGC 2477.

Finally, inspection of figure 8 reveals a small number of stars which do not fall on or near the major sequences. As these probable field stars constitute only a small fraction of the total number, they have been ignored in the following discussion of the C-M diagram.

b) Gap Analysis

NGC 2477 was the first cluster in which a gap was noted on the evolved main sequence (ES). Since then gaps have been found in other clusters, and recently attempts have been made to deduce the chemical composition of cluster stars by comparing the observed gaps with the results of theoretical model computations (Aizenman, Demarque and Miller 1969; Demarque and Miller 1969). Those authors devised a method for detecting gaps, and we have used their method here.

An infinitely narrow locus was constructed on figure 8 with the aid of the corrected

photoelectric data in figure 7*b*. Stars within ± 0.1 mag in $(B - V)$ were then brought back to this locus along lines with the same slope as the long axis of the error box. In this respect the analysis differed from that of Aizenman *et al.* who used a shallower slope since they had only to contend with random photometric errors. A plot of the number of stars fainter than V against V is shown in figure 9*a*. The steeper line in the same figure shows the results obtained when the corrected photoelectric data were considered separately. (In this case stars were brought back along horizontal lines and a uniform absorption correction of 0.84 mag was applied before plotting in fig. 9.)

In order to determine the statistical significance of the possible gaps we applied the test used by Hawarden (1971) on similar data in other clusters. We drew straight lines through the data on either side of the suspected gap. Using the mean slope S, we calculated the quantity $N = \delta V/S$, where δV is the width of the gap. The quantity $\chi^2 = (N - N_0)^2/N$ is then computed, where N_0 is the actual number of stars observed within δV. From a χ^2 table we found the percentage probability that the suspected gap was fictitious. In figure 9*a* we analyzed two features—one at $V \sim 14$ and the other at $V \sim 13.3$. The results are summarized in table 4. We then applied an identical analysis, shown in figure 9*b*, to the data of ES. This analysis is somewhat less accurate, as the results in figure 9*b* were found by reading directly from figure 2 of ES because these authors did not publish their photographic observations in tabular form. The same two

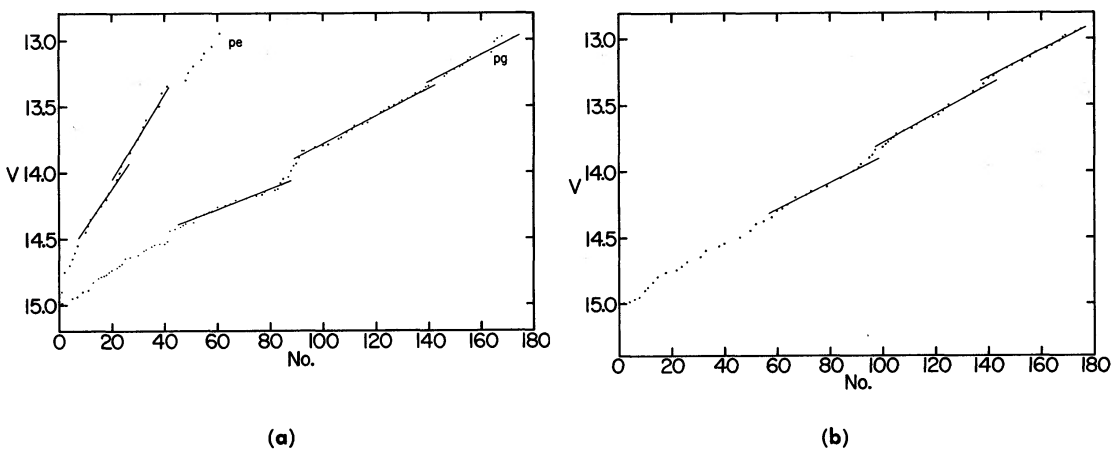

FIG. 9.—(*a*) The luminosity function for the main sequence of NGC 2477 from the photographic and photoelectric data in this paper. The method used for obtaining these functions is explained in the text. There appears to be a deficiency of stars in both pg and pe functions at $13.87 < V < 14.10$ mag. (*b*) A similar luminosity function determined from counting stars in ES's published C-M diagram. It also shows the same deficiency of stars near $V \sim 14.0$ mag.

TABLE 4

SUMMARY OF GAP ANALYSIS

Source of Data	Feature	L^2	% Probability that Gap Does Not Exist
This paper (pg).....	$V \sim 13.4$	3.2	7
This paper (pg).....	$V \sim 14.0$	12.0	0.05
This paper (pe).....	$V \sim 14.0$	0.96	32
ES (pg).....	$V \sim 13.4$	3.0	8
ES (pg).....	$V \sim 13.8$	4.3	3.6

features were analyzed and their results are also listed in table 4. Giving lower weight to the analysis of the photoelectric data due to the small number of stars we conclude from table 4 that the feature near $V \sim 14$ in figure 9 is real.

c) Distance Modulus

Our photoelectrically calibrated photographic observations extend nearly 4 mag below the turnoff point, enabling a distance modulus based on main-sequence superposition to be made. We determined the reddening of stars plotted in figure 8 to be $E_{B-V} = 0.28 \pm 0.05$ mag. The unevolved main sequence is reached at $V = 15.0 \pm 0.15$ where $(B - V) = 0.68$. Correcting for reddening yields $V_0 = 14.16$ at $(B - V)_0 = 0.40$. Superposing on the zero-age main sequence (Eggen 1965), we find $(m - M)_0 = 10.61 \pm 0.21$.

d) Age

In order to determine the age of NGC 2477 we require a set of theoretical evolutionary tracks with turnoff luminosities around $1.5 \leq M_{\text{bol}} \leq 2.5$. We used the tracks of Hallgren and Demarque (1966) and Hallgren (1967) which were computed for $X = 0.67$, $Z = 0.03$. In order to make the comparison with our observations, we plotted the computed tracks on the (M_{bol}, time)-plane and drew in loci where (*a*) core hydrogen exhaustion begins, (*b*) hydrogen shell burning begins, and (*c*) the tracks reach their maximum brightness. In this diagram, shown in figure 10, isochrones are represented by vertical lines. The turnoff point is not well defined in figure 7*b*. For this reason we have plotted on figure 10 the apparent position of the gap found in the previous section. With $E_{B-V} = 0.28$, $(m - M)_0 = 10.61$ and B.C. = 0 (Morton and Adams 1968) we read off from figure 10 ages of $1.54 \pm 0.2 \times 10^9$ and $1.51 \pm 0.2 \times 10^9$ years from the upper and lower edges of the gap. We conclude that the turnoff occurs at $V_0 \sim 12.75$ and that the maximum extent of the isochrone is approximately $V_0 \sim 12.45$.

We further conclude that the break found from our gap analysis around $V \sim 13.3$

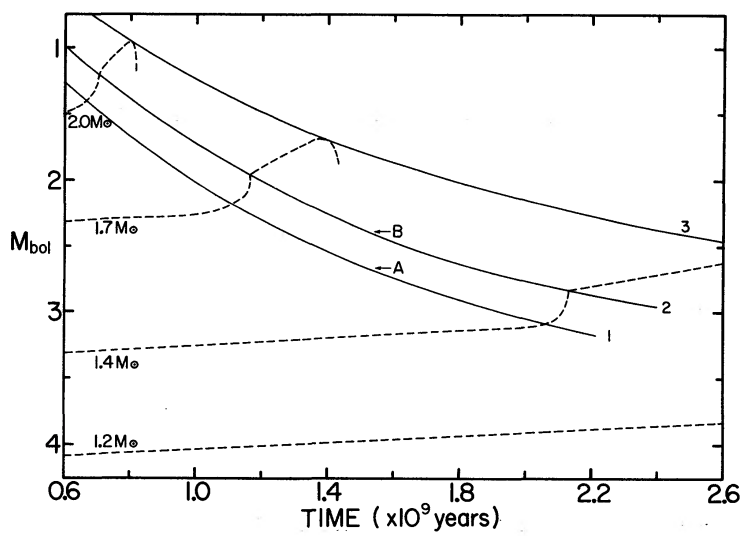

FIG. 10.—The theoretical tracks (*dashed lines*) of Hallgren (1967) and Hallgren and Demarque (1966), plotted on the (M_{bol}, time)-plane. The solid curves show the loci of points where (1) hydrogen exhaustion occurs in the convective core, (2) shell burning begins, and (3) the tracks reach maximum luminosity. This diagram is useful since isochrones are vertical straight lines. At the luminosity where the slope of the tracks becomes steep, a deficiency of stars should be found in the C-M diagram. From the luminosity of this deficiency found in fig. 9*a* (indicated by points A and B in this figure), the age of the cluster can be estimated at 1.5×10^9 years. Using this age, the maximum luminosity of the isochrone can be predicted, giving the turnoff shown by the solid curve in the C-M diagram of figure 7*b*.

separates the actual isochrone from a distinct group of stars lying above the turnoff. Regarding this group of stars, we note that this clump of stars appears anomalous in figure 7 as if it were a brighter turnoff and as the beginning of a blue-straggler sequence. Further, we note that this group occupies an anomalous position in the two-color diagram (fig. 5); i.e., although they appear to fall on an extension of the Hyades main sequence in the C-M diagram, they occupy the low-gravity region of the two-color diagram (Eggen and Sandage 1964: figs. 4 and 5). Such stars may be analogous to those found in NGC 188 by Eggen and Sandage (1969), who plotted those stars as open triangles in their figure 1. Similar, but less populated, clumps of stars appear above the turnoffs in the C-M diagrams of other intermediate-age clusters, such as NGC 7789 (Burbidge and Sandage 1958) and NGC 2158 (Arp and Cuffey 1962).

In concluding this section, we note that the age we have derived for NGC 2477 is subject to revision when new tracks with recent opacities for $Z \sim 0.05$ become available in this mass range.

V. SUMMARY

This photometric study of NGC 2477 has yielded the following properties of the cluster: (1) From DDO photometry of the giants and *UBV* photometry of the main-sequence stars we find a differential reddening ranging from $E_{B-V} = 0.2$ to $E_{B-V} \sim 0.4$ mag. (2) From DDO photometry of the giants we find a relative metallicity of $\sim$1.5 times that of the Hyades, a value consistent with *UBV* photometry of the main-sequence stars. (3) A gap analysis using the method of Aizenman *et al.* (1968) has revealed a deficiency of stars on the evolved main sequence with apparent magnitude $13.87 < V < 14.10$. (4) Using the main-sequence-fitting method, we have found a true distance modulus of $(m - M)_0 = 10.61 \pm 0.21$. (5) A comparison of our C-M diagram with the theoretical models of Hallgren and Demarque (1966) and Hallgren (1967) yields an age of $1.5 \pm 0.2 \times 10^9$ years for NGC 2477. (6) Based on the above interpretation of the C-M diagram, we have found a group of stars resembling a brighter turnoff with apparently lower surface gravities than main-sequence stars lying above and blueward of the turnoff point. An apparently similar group of stars was found by Eggen and Sandage (1969) in NGC 188.

We wish to thank Mrs. M. Reeve who made many of the photographic observations and the Night Assistants at Cerro Tololo for their excellent help. One of us (F. D. A. H.) acknowledges financial support from the University of Victoria and the National Research Council of Canada. We are also grateful to the National Science Foundation for its support of the Cerro Tololo Inter-American Observatory.

REFERENCES

Aizenman, M. L., Demarque, P., and Miller, R. H. 1969, *Ap. J.*, **155**, 973.
Arp, H., and Cuffey, J. 1962, *Ap. J.*, **136**, 51.
Blanco, V. M., Demers, S., Douglass, G. G., and FitzGerald, M. P. 1968, *Pub. U.S. Naval Obs.*, 2d ser., **21**, 1.
Brück, M. T., Smyth, M. J., and McLachlan, A. 1968, *Pub. Roy. Obs. Edinburgh*, **6**, No. 9, p. 209.
Burbidge, E. M., and Sandage, A. 1958, *Ap. J.*, **128**, 174.
Cousins, A. W. J. 1967, *M.N.R.A.S. South Africa*, **26**, 151.
———. 1970, *ibid.*, **29**, 32.
Cousins, A. W. J., Lake, R., and Stoy, R. H. 1966, *R.O.B.*, No. 121.
Cousins, A. W. J., and Stoy, R. H. 1962, *R.O.B.*, No. 49.
———. 1963, *ibid.*, No. 64.
Demarque, P., and Miller, R. H. 1969, *Ap. J.*, **158**, 1037.
Eggen, O. J. 1963, *Ap. J.*, **138**, 356.
———. 1965, *Ann. Rev. Astr. and Ap.*, **3**, 235.
Eggen, O. J., and Sandage, A. 1964, *Ap. J.*, **140**, 130.
———. 1969, *ibid.*, **158**, 669.
Eggen, O. J., and Stoy, R. H. 1961, *R.O.B.*, No. 24 (ES).
Fernie, J. D. 1963, *A.J.*, **68**, 780.

Goodenough, D. G. 1969, unpublished Ph.D. thesis, University of Toronto.
Hallgren, E. L. 1967, *Ap. J.*, **148**, 817.
Hallgren, E. L., and Demarque, P. 1966, *Ap. J.*, **146**, 430.
Hawarden, T. G. 1971, *Observatory*, **91**, 78.
Janes, K. A., and McClure, R. D. 1971, *Ap. J.*, **165**, 561.
Johnson, H. L. 1963, in *Basic Astronomical Data*, ed. K.Aa. Strand (Chicago: University of Chicago Press), p. 204.
Johnson, H. L., and Knuckles, C. F. 1955, *Ap. J.*, **122**, 209.
Johnson, H. L., Mitchell, R. I., Iriarte, B., and Wisniewski, W. Z. 1966, *Comm. Lunar and Planet. Lab.*, **4**, 99.
McClure, R. D. 1970, *A.J.*, **75**, 41.
———. 1971, paper presented at I.A.U. Symp. No. 50.
McClure, R. D., and Bergh, S. van den. 1968, *A.J.*, **73**, 313.
McClure, R. D., and Racine, R. 1969, *A.J.*, **74**, 1000.
Morton, D. C., and Adams, T. F. 1968, *Ap. J.*, **151**, 611.
Roman, N. G. 1952, *Ap. J.*, **116**, 122.
Schmidt-Kaler, T. 1961, *Astr. Nach*, **286**, 113.
Wallerstein, G. 1962, *Ap. J. Suppl.*, **6**, 407.
Wallerstein, G., and Helfer, H. L. 1966, *A.J.*, **71**, 350.
Wildey, R. L. 1963, *A.J.*, **68**, 190.